ACTA MECHANICA SINICA, Vol.20, No.5, October 2004
The Chinese Society of Theoretical and Applied Mechanics
Chinese Journal of Mechanics Press, Beijing, China
Allerton Press, INC., New York, U.S.A.

ISSN 0567-7718

MESHLESS METHOD BASED ON COLLOCATION WITH CONSISTENT COMPACTLY SUPPORTED RADIAL BASIS FUNCTIONS*

SONG Kangzu(宋康祖) ZHANG Xiong (张 雄)† LU Mingwan (陆明万)

(*Department of Engineering Mechanics, Tsinghua University, Beijing* 100084, *China*)

ABSTRACT: Based on our previous study, the accuracy of derivatives of interpolating functions are usually very poor near the boundary of domain when Compactly Supported Radial Basis Functions (CSRBFs) are used, so that it could result in significant error in solving partial differential equations with Neumann boundary conditions. To overcome this drawback, the Consistent Compactly Supported Radial Basis Functions (CCSRBFs) are developed, which satisfy the predetermined consistency conditions. Meshless method based on point collocation with CCSRBFs is developed for solving partial differential equations. Numerical studies show that the proposed method improves the accuracy of approximation significantly.

KEY WORDS: radial basis function, collocation, meshless

1 INTRODUCTION

During recent years, much attention has been paid to the development of meshless methods, and about 10 different meshless methods have been developed, such as the Smooth Particle Hydrodynamics (SPH)[1], the Diffuse Element Method (DEM)[2], the Element Free Galerkin Method (EFG)[3], the Reproducing Kernel Particle Method (RKPM)[4], the Finite Point Method (FP)[5], the hp Clouds Method (HP)[6], the Meshless Local Petrov-Galerkin method (MLPG)[7], the Local Boundary Integral Equation method (LBIE)[8], the Radial Basis Functions method (RBF)[9], RBF-type meshfree boundary techniques[10,11], Least Square Collocation Meshless method (LSCM)[12], and several others.

In those meshless methods, there are mainly four different ways to construct approximation functions entirely in terms of points, namely, smooth particle hydrodynamics method (SPH), moving least square method(MLS), partition of unity method, and radial basis functions (RBF). All of them discretize the domain of interest by using a set of scattered points, and establish the shape functions at the global level without the requirement of any mesh.

The multivariate functions $\varphi(\cdot) : R^d \to R$ can be efficiently evaluated if they are expressible as univariate functions $\varphi(\cdot) = \phi(\|\cdot\|)$ of the Euclidean norm $\|\cdot\|$ in R^d, and such functions are called Radial Basis Functions (RBFs). The RBFs have been successfully developed for interpolation, and a typical construction of interpolations with a set of scattered points $\boldsymbol{x}_i, 1 \le i \le N$, is given by

$$u^h(\boldsymbol{x}) = \sum_{i=1}^{N} u_i \cdot \phi(\|\boldsymbol{x} - \boldsymbol{x}_i\|) \tag{1}$$

Point collocation method with RBFs to solve PDEs is a truly mesh-free method, and possesses many advantages. However, RBFs are generally globally supported and poorly conditioned. Although there are several remedies for these problems, such as domain decomposition, preconditioning, and fine tuning of the variable parameter of RBFs, the compactly supported RBFs (CSRBFs) provide a promising approach[13~15]. If CSRBFs are used, the evaluation of (1) will not run over whole set of N summands and the coefficient matrix will be sparse. Wu[13] provided criteria for positive definiteness of CSRBFs and produced a series of positive definite and compactly

Received 20 December 2001, revised 27 February 2004
* The project supported by the National Natural Science Foundation of China (10172052)
† E-mail: xzhang@tsinghua.edu.cn

supported radial basis functions. Wendland[14] and Buhmann[15] also proposed several CSRBFs. Two classes of compactly supported positive definite RBFs will be studied in this paper, namely

$$\begin{aligned}&\text{CSRBF1}^{[13]}:\ \phi(r)=(1-r)_+^6(6+36r+82r^2+\\&\quad 72r^3+30r^4+5r^5)\in C^4\cap PD_3\\&\text{CSRBF2}^{[14]}:\ \phi(r)=(1-r)_+^8(32r^3+25r^2+\\&\quad 8r+1)\in C^6\cap PD_3\end{aligned}\tag{2}$$

where $r=\|\boldsymbol{x}-\boldsymbol{x}_0\|/R$, in which $\boldsymbol{x}_0$ is the center of the CSRBF, R is the radius of the compactly supported domain. PD_d represents the fact that the radial function is positive definite in $\boldsymbol{R}^d$, and $(1-r)_+$ is given by

$$(1-r)_+=\begin{cases}(1-r) & \text{if } 0\le r\le 1\\ 0 & \text{otherwise}\end{cases}\tag{3}$$

The meshless methods based on point collocation with CSRBFs were studied in our previous work[9]. It was shown that the accuracy of derivatives of the interpolating functions are usually very poor near the boundary of domain, therefore, it will result in significant error in solving a PDE with Neumann boundary conditions. The method of Hermit type collocation was proposed, which can improve the accuracy significantly. However, the numerical studies also demonstrated some shortcomings of the CSRBFs. The accuracy of the solutions is much lower than those using globally supported RBFs, and the acceptable accuracy can only be obtained by using large support size. To overcome these shortcomings, the consistent compactly supported radius basis functions (CCSRBFs) are proposed in this paper, which are not only compactly supported but also satisfy the predetermined consistency conditions. Based on the point collocation with CCSRBFs, the meshless method is then developed. As a test on the proposed method, the interpolation, Poisson equation, and some problems in elasto-statics are studied in detail. Numerical examples show that the present method improves the accuracy significantly.

2 CONSISTENT COMPACTLY SUPPORTED RADIAL BASIS FUNCTIONS

In general, with a set of scattered nodes $\boldsymbol{x}_i,(i=1,2,\cdots,N)$, the original CSRBFs $\phi(\boldsymbol{x})$ do not satisfy the 0th-order consistency, namely

$$\sum_{i=1}^{N}\phi_i(\boldsymbol{x})\neq 1\tag{4}$$

which means that it is even unable to reproduce constant function exactly by using Eq.(1). It can also be shown that the CSRBFs do not satisfy the kth-order consistency, so that it is unable to reproduce kth-order polynomials exactly.

Let $\tilde{\phi}_i^{(0)}$, $\tilde{\phi}_i^{(1)}$ and $\tilde{\phi}_i^{(2)}$ denote CCSRBFs that satisfy the 0th-order, 1st-order and 2nd-order consistency, respectively, namely

$$\sum_{i=1}^{N}\tilde{\phi}_i^{(0)}(\boldsymbol{x})=1\tag{5}$$

$$\begin{aligned}&\sum_{i=1}^{N}\tilde{\phi}_i^{(1)}(\boldsymbol{x})=1\\&\sum_{i=1}^{N}x_i\cdot\tilde{\phi}_i^{(1)}(\boldsymbol{x})=x\\&\sum_{i=1}^{N}y_i\cdot\tilde{\phi}_i^{(1)}(\boldsymbol{x})=y\end{aligned}\tag{6}$$

$$\begin{aligned}&\sum_{i=1}^{N}\tilde{\phi}_i^{(2)}(\boldsymbol{x})=1\\&\sum_{i=1}^{N}x_i\cdot\tilde{\phi}_i^{(2)}(\boldsymbol{x})=x\\&\sum_{i=1}^{N}y_i\cdot\tilde{\phi}_i^{(2)}(\boldsymbol{x})=y\\&\sum_{i=1}^{N}x_i^2\cdot\tilde{\phi}_i^{(2)}(\boldsymbol{x})=x^2\\&\sum_{i=1}^{N}x_iy_i\cdot\tilde{\phi}_i^{(2)}(\boldsymbol{x})=xy\\&\sum_{i=1}^{N}y_i^2\cdot\tilde{\phi}_i^{(2)}(\boldsymbol{x})=y^2\end{aligned}\tag{7}$$

for a 2D problem. Equations (6) and (7) can also be rewritten as

$$\begin{aligned}&\sum_{i=1}^{N}\tilde{\phi}_i^{(1)}(\boldsymbol{x})=1\\&\sum_{i=1}^{N}(x-x_i)\cdot\tilde{\phi}_i^{(1)}(\boldsymbol{x})=0\\&\sum_{i=1}^{N}(y-y_i)\cdot\tilde{\phi}_i^{(1)}(\boldsymbol{x})=0\end{aligned}\tag{8}$$

$$\begin{aligned}
&\sum_{i=1}^{N}\tilde{\phi}_i^{(2)}(\boldsymbol{x})=1\\
&\sum_{i=1}^{N}(x-x_i)\tilde{\phi}_i^{(2)}(\boldsymbol{x})=0\\
&\sum_{i=1}^{N}(y-y_i)\tilde{\phi}_i^{(2)}(\boldsymbol{x})=0\\
&\sum_{i=1}^{N}(x-x_i)^2\tilde{\phi}_i^{(2)}(\boldsymbol{x})=0\\
&\sum_{i=1}^{N}(x-x_i)(y-y_i)\tilde{\phi}_i^{(2)}(\boldsymbol{x})=0\\
&\sum_{i=1}^{N}(y-y_i)^2\tilde{\phi}_i^{(2)}(\boldsymbol{x})=0
\end{aligned}\tag{9}$$

The CCSRBF $\tilde{\phi}_i^{(k)}(\boldsymbol{x})$ can be derived from $\phi_i(\boldsymbol{x})$ given in Eq.(2) by

$$\tilde{\phi}_i^{(k)}(\boldsymbol{x})=\phi_i(\boldsymbol{x})\boldsymbol{p}_i^{\mathrm{T}}(\boldsymbol{x})\cdot\boldsymbol{b}(\boldsymbol{x})\tag{10}$$

where $\boldsymbol{b}^{\mathrm{T}}(\boldsymbol{x})$ is a vector of coefficients to be evaluated, which as indicated, are functions of the spatial coordinates $\boldsymbol{x}$, and

$$\boldsymbol{p}_i^{\mathrm{T}}(\boldsymbol{x})=\begin{cases}[1] & \text{for } k=0\\ [1,\ x-x_i,\ y-y_i] & \text{for } k=1\\ [1,\ x-x_i,\ y-y_i,\ (x-x_i)^2,\\ \quad (x-x_i)(y-y_i),\ (y-y_i)^2] & \text{for } k=2\end{cases}\tag{11}$$

Substituting Eq.(10) into Eq.(8) or Eq.(9) yields

$$\boldsymbol{M}\cdot\boldsymbol{b}=\boldsymbol{q}\tag{12}$$

where

$$\boldsymbol{M}=\sum_{i=1}^{N}\phi_i(\boldsymbol{x})\boldsymbol{p}_i(\boldsymbol{x})\boldsymbol{p}_i^{\mathrm{T}}(\boldsymbol{x})$$

$$\boldsymbol{q}=[1,0,0,0,0,0]^{\mathrm{T}}$$

Solving Eq.(12) for $\boldsymbol{b}$, and substituting it into Eq.(10), one obtains

$$\tilde{\phi}_i^{(k)}(\boldsymbol{x})=\phi_i(\boldsymbol{x})\boldsymbol{p}_i^{\mathrm{T}}(\boldsymbol{x})\boldsymbol{M}^{-1}\boldsymbol{q}\tag{13}$$

The function $u(\boldsymbol{x})$ can be approximated by using CCSRBF $\tilde{\phi}_i^{(k)}(\boldsymbol{x})$ as

$$u(\boldsymbol{x})\approx u^h(\boldsymbol{x})=\sum_{i=1}^{N}u_i\cdot\tilde{\phi}_i^{(k)}(\boldsymbol{x})\tag{14}$$

Clearly, the CCSRBFs $\tilde{\phi}_i^{(0)}(\boldsymbol{x})$ are identical to the well-known Shepard functions, namely

$$\tilde{\phi}_i^{(0)}(\boldsymbol{x})=\frac{\phi_i(\boldsymbol{x})}{\sum_{i=1}^{N}\phi_i(\boldsymbol{x})}\tag{15}$$

In the following sections, prefix of "C0_", "C1_" and "C2_" will be used to denote the 0th-order, 1st-order and 2nd-order consistency, respectively. For example, "C2_CSRBF1" denotes the CCSRBF which is derived from CSRBF1 given in Eq.(2) and satisfies the 2nd-order consistency.

To show the difference between CSRBFs and CCSRBFs, the domain $x\in[0,20]$ is discretized by 21 regular nodes, and the CSRBF1 defined in Eq.(2) with the support size $R=2.5$ is chosen as the original radial basis function. Figure 1 shows the shape of the CSRBF1, C1_CSRBF1 and C2_CSRBF1 for the node at $x=10$, while Fig.2 shows their derivatives.

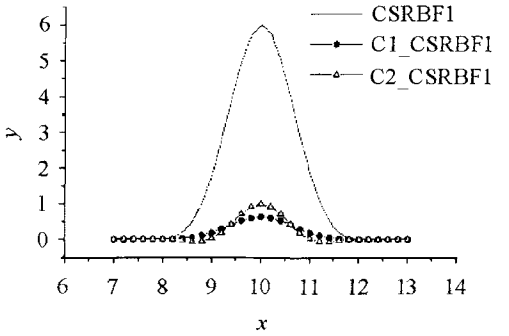

Fig.1 The shape of basis function at $x=10$

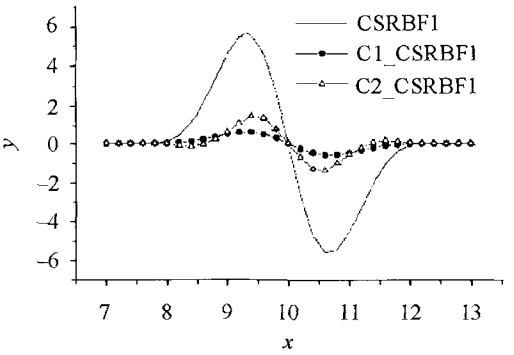

Fig.2 The derivative of basis function at $x=10$

3 MESHLESS METHOD BASED ON POINT COLLOCATION WITH CCSRBFS FOR LINEAR ELASTICITY

Consider the 2D linear elasto-statics governed by a differential equation

$$\boldsymbol{A}\cdot\boldsymbol{\sigma}(\boldsymbol{x})+\boldsymbol{f}(\boldsymbol{x})=0\qquad\boldsymbol{x}\in\Omega\tag{16}$$

$$\boldsymbol{u}(\boldsymbol{x}) = \bar{\boldsymbol{u}}(\boldsymbol{x}) \qquad \boldsymbol{x} \in \Gamma_u \tag{17}$$

$$\boldsymbol{n} \cdot \boldsymbol{\sigma}(\boldsymbol{x}) = \bar{\boldsymbol{t}}(\boldsymbol{x}) \qquad \boldsymbol{x} \in \Gamma_t \tag{18}$$

where $\bar{\boldsymbol{u}}$ is the prescribed displacement on the essential boundary Γ_u, and $\bar{\boldsymbol{t}}$ is the prescribed traction on the natural boundary Γ_t,

$$\boldsymbol{A} = \begin{bmatrix} \dfrac{\partial}{\partial x} & 0 & \dfrac{\partial}{\partial y} \\ 0 & \dfrac{\partial}{\partial y} & \dfrac{\partial}{\partial x} \end{bmatrix}$$

$$\boldsymbol{n} = \begin{bmatrix} l & 0 & m \\ 0 & m & l \end{bmatrix}$$

$$\boldsymbol{\sigma} = [\sigma_{xx} \quad \sigma_{yy} \quad \tau_{xy}]^{\mathrm{T}}$$

$$\boldsymbol{u} = [u \quad v]^{\mathrm{T}}$$

and l, m are the direction cosines of the outward normal direction of boundary Γ_t. Equations (16)~(18) can be expressed in displacement vector $\boldsymbol{u}$ as

$$\boldsymbol{B} \cdot \boldsymbol{u}(x,y) = -\boldsymbol{f}(x,y) \qquad \text{in } \Omega \tag{19}$$

$$\boldsymbol{u}(x,y) = \bar{\boldsymbol{u}}(x,y) \qquad \text{on } \Gamma_u \tag{20}$$

$$\boldsymbol{T} \cdot \boldsymbol{u}(x,y) = \bar{\boldsymbol{t}}(x,y) \qquad \text{on } \Gamma_t \tag{21}$$

where

$$\boldsymbol{B} = \frac{E_0}{1-\nu_0^2} \cdot \begin{bmatrix} \dfrac{\partial^2}{\partial x^2} + \dfrac{1-\nu_0}{2}\dfrac{\partial^2}{\partial y^2} & \dfrac{1+\nu_0}{2}\dfrac{\partial^2}{\partial x \partial y} \\ \dfrac{1+\nu_0}{2}\dfrac{\partial^2}{\partial x \partial y} & \dfrac{\partial^2}{\partial y^2} + \dfrac{1-\nu_0}{2}\dfrac{\partial^2}{\partial x^2} \end{bmatrix}$$

$$\boldsymbol{T} = \frac{E_0}{1-\nu_0^2} \cdot \begin{bmatrix} l\dfrac{\partial}{\partial x} + m\dfrac{1-\nu_0}{2}\dfrac{\partial}{\partial y} & l\nu_0\dfrac{\partial}{\partial y} + m\dfrac{1-\nu_0}{2}\dfrac{\partial}{\partial x} \\ m\nu_0\dfrac{\partial}{\partial x} + l\dfrac{1-\nu_0}{2}\dfrac{\partial}{\partial y} & m\dfrac{\partial}{\partial y} + l\dfrac{1-\nu_0}{2}\dfrac{\partial}{\partial x} \end{bmatrix}$$

in which $E_0 = E$, $\nu_0 = \nu$ for plane stress, and $E_0 = \dfrac{E}{1-\nu^2}$, $\nu_0 = \dfrac{\nu}{1-\nu}$ for plane strain.

Using the consistent compactly supported radial basis functions, the displacement vector $\boldsymbol{u}(x,y)$ can be approximated by a set of scattered nodes $\boldsymbol{x}_i, i = 1, 2, \cdots, N$, as

$$\begin{aligned} u(x,y) &= \sum_{i=1}^{N} u_i \cdot \tilde{\phi}_i^k(\boldsymbol{x}) \\ v(x,y) &= \sum_{i=1}^{N} v_i \cdot \tilde{\phi}_i^k(\boldsymbol{x}) \end{aligned} \tag{22}$$

where $\tilde{\phi}_i^k(\boldsymbol{x})$ is a CCSRBF satisfying kth-order consistency, and u_i, v_i are coefficients to be determined.

Two methods of discretization, namely, the collocation method and Galerkin method, have been dominant in the existing meshless methods. Although Galerkin method possesses several advantages, one of the major difficulties in the implementation of Galerkin-based meshless methods is how to evaluate integrals in the weak form. Nodal integration, cell or octree quadrature, and background finite element mesh quadrature[16] have been used. The first of these is the fastest, but appears to suffer from instability and several stabilization schemes have been developed. The second and third have the disadvantage that the resulting method is not truely meshless. In Galerkin method, derivatives in domain integrals are lowered by using the divergence theorem to establish the weak form. The inaccuracy in integration will result in significant error in the solution. However, the shape functions in meshless method are very complicated. Delicate background cells and a large number of quadrature points must generally be employed to integrate the weak form as accurate as possible. As a consequence, the Galerkin-based meshless methods are much more expensive than FEM. In contrast, collocation-based meshless methods are truly meshless and very efficient.

In a point collocation approach, Eqs.(19)~(21) are satisfied at every point or node. For a node that is in the interior and is not constrained, the collocation approach satisfies the equation

$$\boldsymbol{B} \cdot \boldsymbol{u}(\boldsymbol{x}_i) = -\boldsymbol{f}(\boldsymbol{x}_i) \qquad i = 1, 2, \cdots, N_\Omega \tag{23}$$

For points that are constrained by a Dirichlet boundary condition, the point collocation technique satisfies

$$\boldsymbol{u}(\boldsymbol{x}_i) = \bar{\boldsymbol{u}}(\boldsymbol{x}_i) \qquad i = 1, 2, \cdots, N_u \tag{24}$$

and for points with Neumann boundary conditions, the following equation is satisfied

$$\boldsymbol{T} \cdot \boldsymbol{u}(\boldsymbol{x}_i) = \bar{\boldsymbol{t}}(\boldsymbol{x}_i) \qquad i = 1, 2, \cdots, N_t \tag{25}$$

In Eqs.(23)~(25), N_Ω is the total number of nodes located in the domain Ω, N_u is the total number of nodes located on the Dirichlet boundary Γ_u, and N_t is the total number of nodes located on the Neumann boundary Γ_t, and $N = N_\Omega + N_u + N_t$.

$2N$ linear equations are obtained from Eqs.(23)~(25) which will be used to solve u_i and v_i $(i = 1, 2, \cdots, N)$.

Note that the prescribed traction conditions (25) must be explicitly implemented even on traction-free boundaries. This is quite different to the Galerkin method, in which traction-free boundaries require no calculation of boundary integrals.

The application of a point collocation method is very straightforward when compared to a Galerkin method. The Galerkin method requires the construction of a weak form and the evaluation of the integrals arising in the weak-form is typically expensive. Since a weak form is not constructed in a point collocation approach, the issue of a background mesh does not arise. The imposition of boundary conditions in a Galerkin-based meshless method is considered as a major challenge. The imposition of boundary conditions is, however, very straightforward without any difficulty when a point collocation method is applied. But, the coefficient matrix in a point collocation method is generally non-symmetric, and also requires the calculation of second order derivatives, which are, typically, not required in a Galerkin-based meshless method.

4 NUMERICAL EXAMPLES

4.1 Poisson Equation

The Poisson equation

$$\begin{aligned} &\Delta u(x,y) = -2(x + y - x^2 - y^2) \\ &\text{in } \Omega : x \in [0,1], \qquad y \in [0,1] \\ &u(x,y) = 0.0 \qquad \text{on } \partial\Omega \end{aligned} \tag{26}$$

is studied first. The exact solution of this equation is given by

$$u(x,y) = (x - x^2)(y - y^2)$$

This problem is analyzed for a 15×15 regular and an irregular node discretization as shown in Fig.3, respectively. To evaluate the accuracy of the solution $u^h(x,y)$, two kinds of relative error norm are defined as

$$U_2 = \frac{\sqrt{\sum_{k=1}^{N} \left[u^h(\boldsymbol{x}_k) - u(\boldsymbol{x}_k)\right] \cdot \left[u^h(\boldsymbol{x}_k) - u(\boldsymbol{x}_k)\right]}}{\sqrt{\sum_{k=1}^{N} u(\boldsymbol{x}_k) \cdot u(\boldsymbol{x}_k)}} \times 100\% \tag{27}$$

$$E_2 = \frac{\sqrt{\sum_{k=1}^{N} \left[\mathrm{d}\boldsymbol{u}^h(\boldsymbol{x}_k) - \mathrm{d}\boldsymbol{u}(\boldsymbol{x}_k)\right]^{\mathrm{T}} \cdot \left[\mathrm{d}\boldsymbol{u}^h(\boldsymbol{x}_k - \mathrm{d}\boldsymbol{u}(\boldsymbol{x}_k)\right]}}{\sqrt{\sum_{k=1}^{N} \left[\mathrm{d}\boldsymbol{u}(\boldsymbol{x}_k)\right]^{\mathrm{T}} \cdot \left[\mathrm{d}\boldsymbol{u}(\boldsymbol{x}_k)\right]}} \times 100\% \tag{28}$$

where $\mathrm{d}\boldsymbol{u} = [u_{,x}, u_{,y}]^{\mathrm{T}}$, $\mathrm{d}\boldsymbol{u}^h = [u^h_{,x}, u^h_{,y}]^{\mathrm{T}}$.

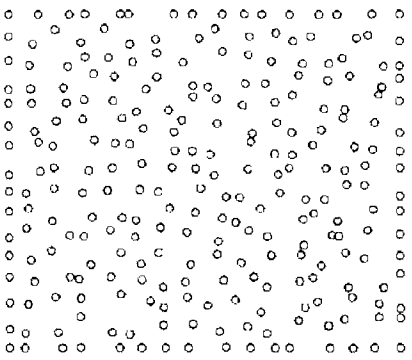

Fig.3 Randomly discributed 256 nodes discretization

The numerical results obtained for the regular and irregular node discretization by using the point collocation with C0_CSRBF, C1_CSRBF and C2_CSRBF are listed in Tables 1 and 2. The results obtained by using CSRBF[9] are also included for the purpose of comparison. This study shows that the CCSRBFs perform much better than CSRBFs, and even CCSRBF with 0th-order consistency can give results with satisfactory accuracy.

Table 1 Relative error of the Poisson equation with regular nodes discretization (%)

	R	CSRBF1	C0_CSRBF1	C1_CSRBF1	C2_CSRBF1
U_2	0.2	28.1	4.82	5.02	0.056 5
	0.25	12.1	1.24	0.04	0.019 8
	0.3	4.49	0.827	0.191	0.031 8
	0.35	2.66	0.489	0.247	0.055 3
E_2	0.2	41.4	19.9	5.61	0.435
	0.25	27.5	9.48	0.394	0.087 4
	0.3	19.5	4.85	0.781	0.308
	0.35	15.3	2.59	0.578	0.398

Table 2 Relative error of the Poisson equation with irregular nodes discretization (%)

	R	CSRBF1	C0_CSRBF1	C1_CSRBF1	C2_CSRBF1
U_2	0.2	54.5	3.18	8.81	9.12
	0.25	21.5	0.93	2.90	0.967
	0.3	7.44	0.43	1.54	0.722
	0.35	3.75	0.328	0.653	0.429
E_2	0.2	61.4	22.0	10.7	22.9
	0.25	32.1	10.0	4.45	3.20
	0.3	19.4	5.02	2.69	3.43
	0.35	14.6	2.89	1.48	4.48

4.2 Cantilever Beam

Consider a Cantilever beam subject to end load as shown in Fig.4. The analytical solution is given by Timoshenko and Goodier[17]. This problem is solved for elastic modulus $E = 1.0 \times 10^4$, the Poisson's ratio $\nu = \dfrac{1}{3}$, $D = 2$ and $L = 12$. The exact displacements are prescribed as essential boundary conditions at $x = 0$, $0 \leq y \leq D$, and the rest of the boundaries are treated as prescribed traction boundaries.

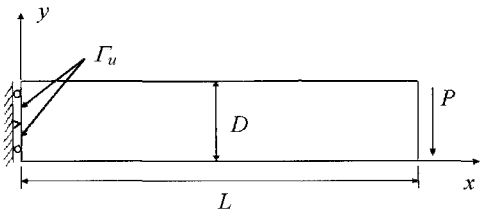

Fig.4 Cantilever beam

To verify the accuracy of the numerical solution, two kinds of relative error norm are evaluated in the form of displacements and stresses, namely

$$L_u = \frac{\sqrt{\sum_{k=1}^{N} \left[\boldsymbol{u}^h(\boldsymbol{x}_k) - \boldsymbol{u}(\boldsymbol{x}_k)\right]^{\mathrm{T}} \cdot \left[\boldsymbol{u}^h(\boldsymbol{x}_k) - \boldsymbol{u}(\boldsymbol{x}_k)\right]}}{\sqrt{\sum_{k=1}^{N} \left[\boldsymbol{u}(\boldsymbol{x}_k)\right]^{\mathrm{T}} \cdot \left[\boldsymbol{u}(\boldsymbol{x}_k)\right]}} \times 100\% \tag{29}$$

$$L_\sigma = \frac{\sqrt{\sum_{k=1}^{N} \left[\boldsymbol{\sigma}^h(\boldsymbol{x}_k) - \boldsymbol{\sigma}(\boldsymbol{x}_k)\right]^{\mathrm{T}} \cdot \left[\boldsymbol{\sigma}^h(\boldsymbol{x}_k) - \boldsymbol{\sigma}(\boldsymbol{x}_k)\right]}}{\sqrt{\sum_{k=1}^{N} \left[\boldsymbol{\sigma}(\boldsymbol{x}_k)\right]^{\mathrm{T}} \cdot \left[\boldsymbol{\sigma}(\boldsymbol{x}_k)\right]}} \times 100\% \tag{30}$$

Numerical solutions are obtained by using regular discretization with 18×3, 24×4, 30×5 and 36×6 nodes, which are listed in Table 3.

Table 3 Relative error norm for Cantilever beam (%)

		18×3	24×4	30×5	36×6
CSRBF1	L_u	99.464	100.06	100.03	100.12
	L_σ	309.06	108.16	105.42	109.02
C1_CSRBF1	L_u	45.904	24.019	21.040	6.861 3
	L_σ	53.475	22.278	22.108	11.557
C2_CSRBF1	L_u	16.821	14.405	9.219 2	1.389 4
	L_σ	19.188	15.752	9.963 2	2.028 7

4.3 Plate with a Hole

Consider the problem of an infinite plate with a central circular hole of radius a centered at the origin, and uniaxially loaded at infinity by a traction σ_0 in the x direction. Due to twofold symmetry, only the first quadrant is modeled. The modeled region extends to the boundaries $x = 5$ and $y = 5$, along which the exact tractions or displacements are applied as prescribed boundary conditions. The radius of the circle is $a = 1$.

Two cases are analyzed here. In the first case, the exact displacements are applied at all boundary nodes, while in the second case, the displacements are only applied at the left and lower edges, and the tractions associated with the exact stress field are applied at the upper and right edges. In the second case, the inner boundary is a traction free boundary. A plane stress state is assumed with material properties $E = 1\,000$ and $\nu = 1/3$. The nodal arrangements used in this example are illustrated in Fig.5.

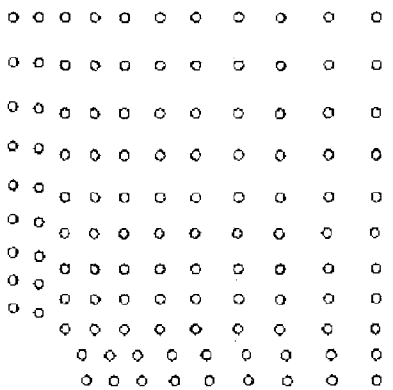

Fig.5 Nodal arrangement for the plate with a central circular hole

This problem is solved with C1_CSRBF1 and C2_CSRBF1, and the relative error norms for cases 1 and 2 are shown in Tables 4 and 5, respectively, the results obtained by using CSRBF1[9] are also included for the purpose of comparison.

Table 4 Relative error norm for case 1 (%)

		$N=48$	$N=117$	$N=352$	$N=513$
CSRBF1	L_u	35.89	42.96	44.71	50.33
	L_σ	136.6	192.9	312.2	344.6
C1_CSRBF1	L_u	1.59	1.312	0.489	0.086
	L_σ	22.46	14.63	5.973	3.338
C2_CSRBF1	L_u	1.167	0.346	0.059 5	0.021
	L_σ	27.88	15.17	3.914	1.703

Table 5 Relative error norm for case 2 (%)

		$N=48$	$N=117$	$N=352$	$N=513$
CSRBF1	L_u	280.47	501.67	332.62	115.27
	L_σ	668.59	1 275.3	2 188.1	675.48
C1_CSRBF1	L_u	88.24	14.855	5.792 8	0.977
	L_σ	316.43	96.737	59.435	3.894
C2_CSRBF1	L_u	31.384	5.481 8	0.835 4	0.342
	L_σ	103.69	15.498	4.138	1.670

5 CONCLUDING REMARKS

Much effort has been made in the development of compactly supported radial basis functions in mathematical communities. However, based on our previous study, reasonable results can be obtained only when the support size of CSRBFs is large enough. The conception of the consistent compactly supported radial basis functions is introduced in this paper, and the method to develop consistent compactly supported radial basis functions from existing CSRBFs to satisfy the predetermined consistency is presented in detail. Numerical studies show that the CCSRBFs can improve the accuracy of approximation significantly.

REFERENCES

1 Gingold RA, Monaghan JJ. Smoothed particle hydrodynamics: theory and applications to non-spherical stars. *Mon Not Roy Astrou Soc*, 1977, 181: 375~389

2 Nayroles B, Touzot G, Villon P. Generalizing the finite element method: diffuse approximation and diffuse elements. *Comput Mech*, 1992, 10: 307~318

3 Belytschko T, Lu YY, Gu L. Element free Galerkin methods. *Int J Numer Methods Engrg*, 1994, 37: 229~256

4 Liu WK, Chen Y, Jun S, et al. Overview and applications of the reproducing kernel particle methods. *Archives of Computational Methods in Engineering*, 1996, 3: 3~80

5 Onate E, Idelsohn S, Zienkiewicz OC, et al. A finite point method in computational mechanics. Applications to convective transport and fluid flow. *Int J Numer Meth Engrg*, 1996, 39: 3839~3866

6 Liszka TJ, Duarte CAM, Tworzydlo WW. hp-meshless cloud method. *Comput Methods Appl Mech Engrg*, 1996, 139: 263~288

7 Atluri SN, Zhu T. A new meshless local Petrov-Galerkin (MLPG) approach in computational mechanics. *Comput Mech*, 1998, 22: 117~127

8 Atluri SN, Sladek J, et al. The Local boundary integral equation (LBIE) and it's meshless implementation for linear elasticity. *Comput Mech*, 2000, 25: 180~198

9 Zhang X, Song KZ, Lu MW. Meshless methods based on collocation with radial basis function. *Comput Mech*, 2000, 26(4): 333~343

10 Chen W. Symmetric boundary knot method. *Engng Anal Bound Elem*, 2002, 26(6): 489~494

11 Chen W. Meshfree boundary particle method applied to Helmholtz problems. *Engng Anal Bound Elem*, 2002, 26(7): 577~581

12 Zhang X, Liu XH, Song KZ, et al. Least square collocation meshless method. *Int J Numer Methods Engrg*, 2001, 51: 1089~1100

13 Wu Z. Compactly supported positive definite radial functions. *Adv Comput Math*, 1995, 4: 283~292

14 Wendland H. Piecewise polynomial, positive definite and compactly supported radial basis functions of minimal degree. *Adv Comput Math*, 1995, 4: 389~396

15 Buhmann MD. Radial functions on compact support. *Proceedings of the Edinburgh Mathematical Society*, 1998, 41: 33~46

16 Belytschko T, Krongauz Y, et al. Meshless methods: an overview and recent developments. *Computer Methods in Applied Mechanics and Engineering*, 1996, 139: 3~47

17 Timoshenko SP, Goodier JN. Theory of Elasticity. 3rd edition. New York: McGraw-Hill, 1987